Pure Appl. Chem., Vol. 74, No. 10, pp. 1909–1920, 2002.

Solid–liquid equilibria in mixtures of molten salt hydrates for the design of heat storage materials*

W. Voigt‡ and D. Zeng

TU Bergakademie Freiberg, Leipziger Strasse 29, D-09596 Freiberg, Germany

Abstract: Enthalpy of melting can be used to store heat in a simple way for time periods of hours and days. Knowledge of the solid–liquid equilibria represents the most important presumption for systematic evaluations of the suitability of hydrated salt mixtures. In this paper, two approaches for predicting solid–liquid equilibria in ternary or higher component systems are discussed using the limited amount of thermodynamic data available for such systems. One method is based on the modified Brunauer–Emmett–Teller (BET) model as formulated by Ally and Braunstein.

In cases of a strong tendency toward complex formation of salt components, the BET model is no longer applicable. Reaction chain models have been used to treat such systems. Thereby, the reaction chain represents a method to correlate step-wise hydration or complexation enthalpies and entropies and, thus, reduce the number of adjustable parameters. Results are discussed for systems containing $MgCl_2$, $CaCl_2$, $ZnCl_2$, and alkali metal chlorides.

INTRODUCTION

Enthalpy of melting can be used to store heat in a simple way for time periods between several hours and days. The storage capacity first of all depends on the volume-specific enthalpy of melting. At temperatures below 423 K, the largest values are found for salt hydrates. Therefore, the technical literature is rich in proposals for heat storage applications with salt hydrates. However, for practical performance besides the heat storage capacity, appropriate melting–crystallization temperatures within a few degrees are crucial for intended applications. Also, reversible phase changes over many heating–cooling cycles have to be ensured, which is easier with congruent melting than with incongruent melting hydrates.

Considering the available pure salt hydrates, selection of suited melting temperatures is quite limited (Table 1). In addition, most of the salt hydrates are incongruently melting, which requires technical measures to reach hydration equilibrium. To increase the number of potential storage materials, mixtures of salt hydrates have to be considered. Knowledge of the solid–liquid equilibria represents the most important presumption for systematic evaluations of the suitability of salt mixtures. Unfortunately, there are only a few detailed experimental investigations of such phase diagrams. Due to the tendency of salt hydrates for supercooling, experimental determinations of liquidus curves are time-consuming. Therefore, modeling of phase diagrams is important for predictions of hydrate mixtures with appropriate melting temperatures as well as for planning of experiments for solid–liquid phase diagram determinations.

*Lecture presented at the 10th International Symposium on Solubility Phenomena, Varna, Bulgaria, 22–26 July 2002. Other lectures are published in this issue, pp. 1785–1920.

‡Corresponding author: E-mail: Wolfgang.Voigt@chemie.tu-freiberg.de

Table 1 Salt hydrates with melting points below 100 °C.

Salt hydrate	Melting temperature	Enthalpy of melting		Melting behavior[a]
	°C	kJ/kg	kJ/dm^3	
$LiClO_3 \cdot 3H_2O$	8	253	approx. 300	c
$K_2HPO_4 \cdot 6H_2O$	13	109	approx. 150	c
$KF \cdot 4H_2O$	18	330	475	c
$CaCl_2 \cdot 6H_2O$	29	170–190	280–290	ic
$LiNO_3 \cdot 3H_2O$	29	298	459	c
$Na_2SO_4 \cdot 10H_2O$	32	244	360	very ic
$Na_2CO_3 \cdot 10H_2O$	33	247	362	very ic
$KFe(SO_4)_2 \cdot 12H_2O$	33	173	240	ic
$LiBr \cdot 2H_2O$	34	124	270	ic
$CaBr_2 \cdot 6H_2O$	34	138	266	not known
$Zn(NO_3)_2 \cdot 6H_2O$	36	130	235	c
$Na_2HPO_4 \cdot 12H_2O$	36	279	424	ic
$FeCl_3 \cdot 6H_2O$	37	223	298	c
$CaCl_2 \cdot 4H_2O$	39	158	250	ic
$Ca(NO_3)_2 \cdot 4H_2O$	42	140	265	c
$KF \cdot 2H_2O$	42	266	441	c
$Fe(NO_3)_3 \cdot 9H_2O$	47	190	300	ic
$Na_2HPO_4 \cdot 7H_2O$	48	140–170	240–290	ic
$Zn(NO_3)_2 \cdot 2H_2O$	55	68	approx. 125	c
$NaCH_3COO \cdot 3H_2O$	58	270–290	358–419	ic
$NaAl(SO_4)_2 \cdot 12H_2O$	61	180	250	ic
$Al(NO_3)_3 \cdot 9H_2O$	70	155–176	270–350	ic
$LiCH_3COO \cdot 2H_2O$	70	150–251	180–301	c
$Na_3PO_4 \cdot 12H_2O$	72	168–221	272–358	very ic
$Na_4P_2O_7 \cdot 10H_2O$	76	230	419	ic
$Ba(OH)_2 \cdot 8H_2O$	78	301	644–656	c
$Al_2(SO_4)_3 \cdot 18H_2O$	88	218	374	ic
$Sr(OH)_2 \cdot 8H_2O$	89	370	700	very ic
$Mg(NO_3)_2 \cdot 6H_2O$	89	160	262	c
$LiCl \cdot H_2O$	99	212	360	ic

[a]c = congruently melting, ic = incongruently melting

DATA ON SOLID–LIQUID EQUILIBRIA

For most binary salt–water systems solid–liquid equilibria are reported until temperatures of approx. 400 K [1,2]. Some examples of phase diagrams for systems {[$LiNO_3$, $Mg(NO_3)_2$, $Ca(NO_3)_2$, $Zn(NO_3)_2$]–H_2O} with relevance to heat storage are given in Fig. 1. These salts form fusible hydrates with melting temperatures included in Table 1. Most of the selected hydrates are congruently melting, which is an advantage in respect to heat storage applications.

Unfortunately, experimental data on polythermal ternary or higher component systems containing molten hydrates are very rare. Besides solubility isotherms at 298 K in a few cases, data at other temperatures are not available. Thermodynamic modeling is required to construct polythermal solid–liquid phase diagrams from such small data sets. The vapor pressure data reported for a limited number of systems are helpful in estimations of model parameters.

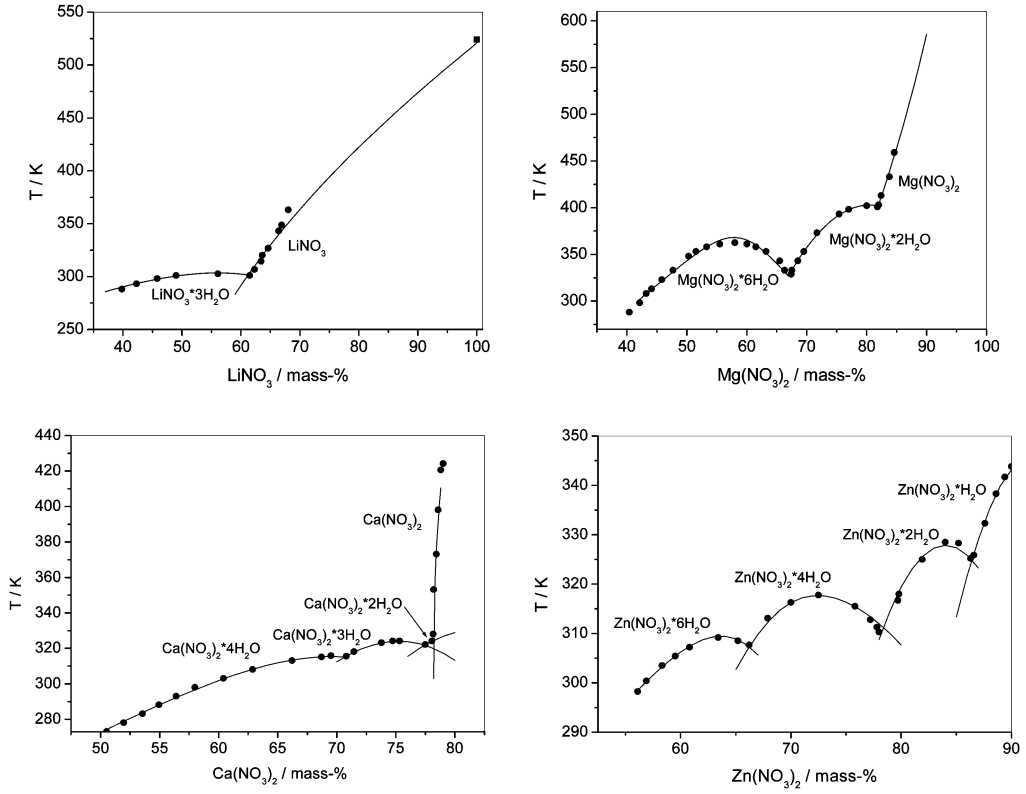

Fig. 1 Selected solid–liquid phase diagrams of binary systems containing fusible salt hydrates. Lines: calculated; symbols: experimental data [2].

MOLTEN HYDRATES

Molten hydrates can be considered as a unique class of aqueous liquids, where most of the water molecules are coordinated at the cations, giving rise to specific properties including low water activity, high acidity, enhanced viscosity, and a tendency for supercooling. On the concentration scale, molten salt hydrates represent a transition region between solutions and molten salts characterized by the dominance of ion–water contact interactions (Fig. 2). For cations like Li^+, Mg^{++}, or Ca^{++}, this situation typ-

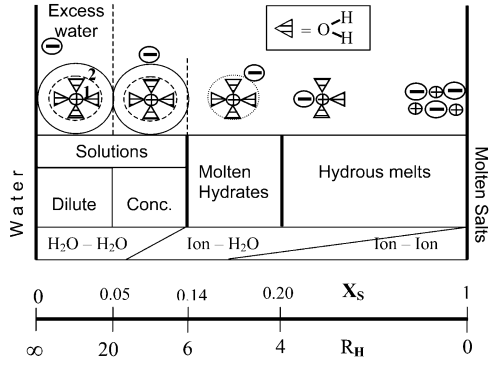

Fig. 2 Characteristic concentration ranges from dilute solutions to molten salts.

ically will exist at molar water/salt ratios R_H = 4–7. In this concentration range, thermodynamic properties can no longer be described by solution models like Pitzer's ion interaction equations [3] without explicit consideration of ion–water interactions. On the other hand, the description of molten hydrates as analogs to molten salts with cations enlarged by the coordinated water sphere represents an oversimplification. Also, quasi-lattice approaches of molten salt mixtures were not successful in this intermediate concentration range between solutions and molten salts [4].

THERMODYNAMIC MODELING OF MOLTEN HYDRATES

BET approach: The model

In 1948, Stokes and Robinson [5] proposed a modified form of the Brunauer–Emmett–Teller (BET) gas adsorption equation to describe the water activity of very concentrated salt solutions by eq. 1.

$$\frac{a_w}{R_H(1-a_w)} = \frac{1}{cr} + \frac{(c-1)a_w}{cr} \tag{1a}$$

$$c = \exp^{\{-\Delta E/RT\}} \tag{1b}$$

The model contains only two adjustable r and ΔE parameters per salt, which is ideal for a situation characterized by a deficiency of data. Parameter r is interpreted as a maximum hydration number of the salt and ΔE as the difference between adsorption energy of water at the salt and condensation energy of pure water. Later, the equation was frequently used to model solvent activities in binary salt–solvent systems [4,6–8]. From all the material, it can be stated that the model is valid only at low solvent activities, mostly below 0.5. Thus, to obtain salt activities, Gibbs–Duhem integration has to be started at the pure molten salt side, which yields an infinite value as can be seen from eq. 2.

$$\int_{\ln a_s(X_w=0)}^{\ln a_s(X_w)} d\ln a_s = -\int_{\ln a_w(x_w=0)}^{\ln a_w} \frac{X_w}{X_s} d\ln a_w \tag{2}$$

where X_w, X_s, a_W, and a_S denote the mole fraction and activity of water and salt.

Introduction of some substitutions of variables and elementary transformations yield an expression, which could be integrated [9]. Braunstein [10] showed that the numerical results from this integration in ref. [9] are identical with those obtained from a formula derived from a 2-dimensional lattice adsorption model.

A simple linear composition dependence of the model parameters was observed for the description of the water activity in ternary systems [11,12]. However, the mathematical form of the resulting BET equations did not allow calculation of activities of each salt component in a direct manner, which is a prerequisite for modeling of ternary phase diagrams. Ally and Braunstein [13] recently extended the statistical lattice model to multicomponent salt systems. According to this model for a ternary system, the number of water molecules X and W occupying sites at salt A and B, respectively, have to be calculated by simultaneously solving equations (eq. 3) at given mole number H of water. Thereafter, these values are used to calculate the water and salt activities a_w, a_A, a_B by inserting X and W into eq. 4.

$$X = \frac{(H-Z)C_A r_A A}{Z+(H-Z)C_A} \tag{3a}$$

$$W = \frac{(H-Z)C_B r_B B}{Z+(H-Z)C_B} \tag{3b}$$

$$Z = X + W \tag{3c}$$

$$a_A = \frac{A}{A+B} * \left(\frac{r_A A - X}{r_A A}\right)^{r_A} \quad (4a)$$

$$a_B = \frac{B}{A+B} * \left(\frac{r_B B - W}{r_B B}\right)^{r_B} \quad (4b)$$

$$a_W = \frac{H - X - W}{H} \quad (4c)$$

All the equations contain only the hydration parameters r and c from the binary subsystems, no additional mixing parameter. The authors [13] tested the model only in the system $LiNO_3$–$LiCl$–H_2O. We used their model to calculate phase diagrams for a series of salt hydrate mixtures with potential interest in heat storage applications.

BET approach: Results

For the example of the system $LiNO_3$–$Mg(NO_3)_2$–H_2O, results are discussed in more detail. Temperature-dependent forms of the parameters r and ΔE (eqs. 5, 6) were taken from [9,14] and are based on vapor pressure data in the binary systems.

$$r(LiNO_3) = 2.8712 - 0.82 \cdot T/1000 \qquad r[Mg(NO_3)_2] = 5.579 \quad (5)$$

$$\Delta E(LiNO_3) = -6.280 + 0.38109 \cdot 0.01 \cdot T \qquad \Delta E[Mg(NO_3)_2] = -0.01348 \cdot T \quad (6)$$

with T in K and ΔE in kJ/mol.

From calculations of water and salt activities along the liquidus curves in the binary systems, temperature-dependent solubility constants K of the solid phases were estimated as given below.

$\ln K = a + b / T$	a	b
$LiNO_3$	4.7358	–2494.80
$LiNO_3 \cdot 3H_2O$	12.8735	–6156.59
$Mg(NO_3)_2$	1.5713	–1504.84
$Mg(NO_3)_2 \cdot 2H_2O$	–5.1480	–2441.48
$Mg(NO_3)_2 \cdot 6H_2O$	–13.8334	–3529.31

Lines in Fig. 1 demonstrate the quality of description in the binary systems. The model was then used to calculate the polythermal solid–liquid equilibria in the ternary system $LiNO_3$–$Mg(NO_3)_2$–H_2O between 273 to 500 K, which are projected in Fig. 3. Available isothermal solubility data at 273 and 298 K (not shown in Fig. 3) coincide with calculated lines. Six eutectic points were found within the ternary system; three represent the stable quasi-binary mixtures

$LiNO_3$–$Mg(NO_3)_2 \cdot 2H_2O$	e1	T = 388 K
$LiNO_3$–$Mg(NO_3)_2 \cdot 6H_2O$	e2	T = 345 K
$LiNO_3 \cdot 3H_2O$–$Mg(NO_3)_2 \cdot 6H_2O$	e3	T = 300 K

The other three eutectics are of ternary type with crystallizing phases

$LiNO_3 + Mg(NO_3)_2 + Mg(NO_3)_2 \cdot 6H_2O$	E1	T = 323 K
$LiNO_3 + LiNO_3 \cdot 3H_2O + Mg(NO_3)_2 \cdot 6H_2O$	E2	T = 300 K
$LiNO_3 + Mg(NO_3)_2 + Mg(NO_3)_2 \cdot 2H_2O$	E3	T = 387 K

The eutectic mixture e2 was already extensively and successful tested as a heat storage material for application in automotives [15]. Its melting point was determined to be at 345 K, which agrees with

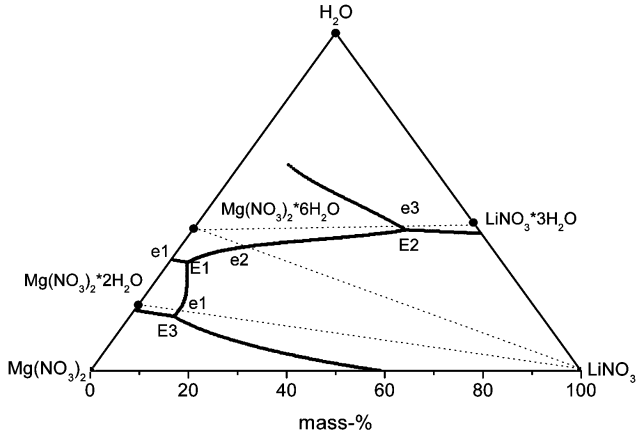

Fig. 3 Polythermal phase diagram of the system $LiNO_3$–$Mg(NO_3)_2$–H_2O. Dotted lines: quasi-binary sections; e1, e2, e3: quasi-binary eutectics; E1, E2, E3: ternary eutectics.

Table 2 List of ternary systems salt (1) – salt (2) – water for which phase diagrams have been predicted by means of the BET model.

Salt component 1	Salt component 2	Salt component 1	Salt component 2
$LiNO_3$	$NaNO_3$	$LiNO_3$	LiCl
$LiNO_3$	$Mg(NO_3)_2$	$LiNO_3$	$LiClO_4$
	$Ca(NO_3)_2$	$LiClO_4$	$Ca(ClO_4)_2$
	$Zn(NO_3)_2$	$Ca(NO_3)_2$	$Ca(ClO_4)_2$
$NaNO_3$	$Mg(NO_3)_2$	LiCl	$MgCl_2$
	$Ca(NO_3)_2$	LiCl	$CaCl_2$
	$Zn(NO_3)_2$		
$Mg(NO_3)_2$	$Ca(NO_3)_2$		
	$Zn(NO_3)_2$		
$Ca(NO_3)_2$	$Zn(NO_3)_2$		

the calculated one. From available vapor pressure and solubility data of a series of binary salt–water systems, BET parameters and solubility constants were estimated and the additive ternary phase diagrams were calculated systematically for ternary systems as listed in Table 2.

The reliability of the predictions was further tested for the system $LiNO_3$–$Ca(NO_3)_2$–H_2O by experimental determinations of liquidus temperatures of an array of 40 samples. The distribution of compositions is plotted in the diagram of Fig. 4A. Crystallization of other hydrates than expected from the binary subsystems should cause corresponding deviations between calculated and experimentally determined liquidus temperatures. In Fig. 4B, the observed deviations are plotted as a function of water content along sections of constant ratios $LiNO_3/Ca(NO_3)_2$. The majority of calculated liquidus temperatures are in agreement with experiment within 3 K.

Mixtures containing other anions than nitrate (chloride, perchlorate) have been modeled in the same way. As an example, the phase diagram of the system LiCl–$MgCl_2$–H_2O is displayed in Fig. 5. Also in this case, available isothermal solubility data coincide with calculations within limits of uncertainty. Generally, it can be concluded that the BET model was successfully applied for systems without pronounced tendencies for complex formation between cations and anions. In systems like LiCl–$ZnCl_2$–H_2O, the simple form of the BET model failed to reproduce experimental data.

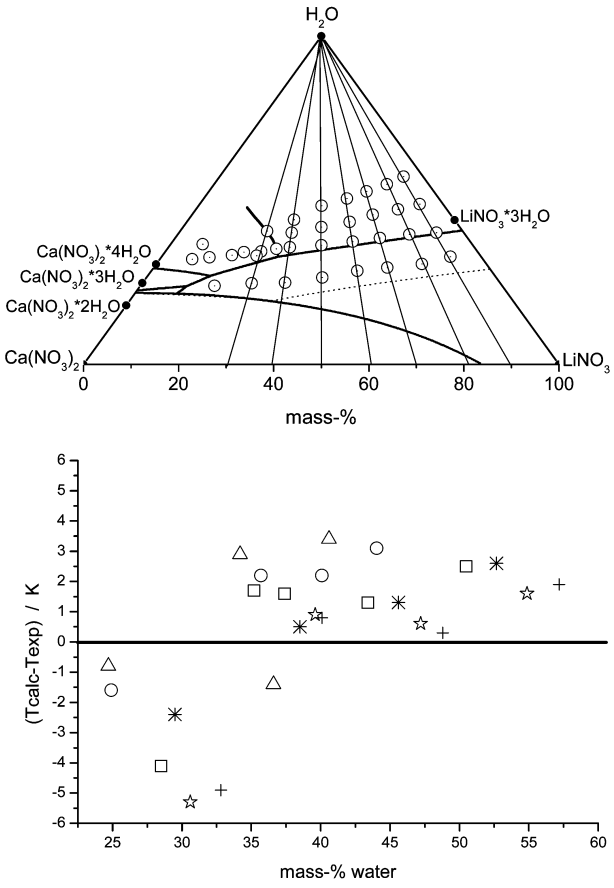

Fig. 4 Experimental determination of liquidus temperatures in the system $LiNO_3$–$Ca(NO_3)_2$–H_2O. (A) Calculated polythermal liquidus curves (thick lines) and distribution of sample compositions, dotted line: calculated solubility isotherm at 373 K; (B) Deviations between calculated and experimental liquidus temperatures.

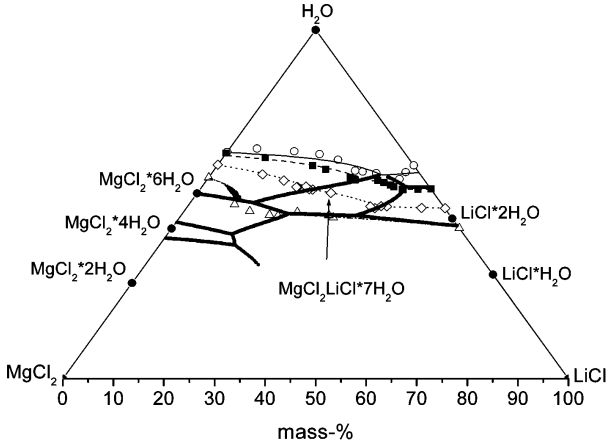

Fig. 5 Phase diagram of the system LiCl–$MgCl_2$–H_2O. Lines = calculated curves, thick: polythermal liquidus curves, thin and interrupted: isothermal solubility curves, symbols = experimental data [2]: (○ 273 K), (■ 298 K), (◇ 343 K), (△ 375 K), (●) composition of solid hydrates.

REACTION CHAIN APPROACH: THE MODEL

Stokes and Robinson [16] showed that the osmotic coefficients of a number of chemically quite different electrolytes can be described up to 30 mol/kg H_2O by means of a step-wise hydration model characterized by only two parameters k, K_1 by means of eq. 1

$$K_i = K_1 \cdot k^{(i-1)} \tag{7a}$$

$$\Delta_R G_i^0 = \Delta_R G_1^0 - RT \cdot (i-1) \cdot \ln k \tag{7b}$$

with K_i as the step-wise equilibrium constant of the ion hydrate including i molecules of water formed from the hydrate containing $(i - 1)$ mol water with i running to the maximum hydration number N. The validity of eq. 7 is supported by mass-spectroscopic determinations of hydration equilibria in the gas phase [21–23]. Following this line, we formulated reaction chains for the formation of hydrated and also complexed ions. Using eq. 7b, the total Gibbs energy of formation of species $Z(X)_n$ according to reaction I is given by eq. 8

$$Z + nX \rightarrow Z(X)_n \tag{I}$$

with $X = H_2O$, Cl^-, etc.

$$\Delta_R G_i = i \cdot \Delta_R G_1 + i \cdot (i - 1)/2 \cdot g \tag{8}$$

Thus, with only two constants $\Delta_R G_1$ and g, the formation of a series of 1 …i…N species is modeled. Analogous equations can be formulated for the formation enthalpies and entropies. Assuming that all changes in Gibbs energy are caused by formation of species and an ideal mixing entropy term, the equilibrium situation is calculated by minimizing the total Gibbs energy of the liquid phase according to eq. 9, subject to mass balances eq. 10

$$G = \sum_{R}^{RC} \sum_{i=1}^{N} (n_i \cdot \Delta_R G_i^0) - T \cdot \Delta_{\text{mix}} S \tag{9}$$

$$\sum_{i=1}^{n} \nu_{i,j} \cdot n_i = N_j \quad (j = \text{basis species}) \tag{10}$$

where summation is performed over all species generated through reaction chains RC. The entropy of mixing is formulated on a volume fraction ϕ_i bases as given in eq. 11, with V_j denoting the volume of species j.

$$\Delta_{\text{mix}} S = -R \sum_{j=1}^{J} (n_j \cdot \log \phi_j) \tag{11a}$$

$$\phi_j = \frac{n_{jVj}}{\sum_{j=1}^{J} n_{jVj}} \tag{11b}$$

For the selection of relevant types of species, as well as for the choice of reasonable magnitudes of parameters, guidance from extra-thermodynamic knowledge, especially from spectroscopy, is necessary. Having the parameters $\Delta_R G_1$, g and n of all reaction chains, available programs like CHEMSAGE [17] or EQ3/6 [18] can be used to calculate the Gibbs energy of solid phases at given experimental solid–liquid phase equilibrium points to extract solubility constants.

Whereas calculations of chemical equilibria involving hundreds of species represent no problem for the codes mentioned above, there exists no ready-to-use software for the reversed task, that is, estimation of sets of interrelated equilibrium constants or Gibbs energies of formation of species from a variety of experimental data sets. After having tested several programs, we used the freely available nonlinear optimization package LANCELOT [19]. This package allows solving of large-scale nonlinear problems including arbitrary constraints on the variables. Also, setting constraints on the magnitudes of model parameters is essential for systematic model development, because the mathematical form of the reaction chain model is numerically very flexible, which yields quite different parameter sets for comparable description quality of experimental data.

Application of the approach will be demonstrated at the system LiCl–$ZnCl_2$–H_2O. This system is characterized by extensive chlorocomplex formation of zinc ions and strong hydration abilities of both Li^+ and Zn^{++}. Solubilities are so high that at room temperature, molar water/salt ratios R_H below 2 are reached.

The water activities, enthalpies of dilution, as well as the phase diagram of the system LiCl–H_2O (Figs. 6A–C) could be described with only one reaction chain

$$LiCl \rightarrow Li(H_2O)^+ \rightarrow \bullet\bullet\bullet\bullet \rightarrow Li(H_2O)_6^+$$

with enthalpy and entropy parameters analogous to eq. 8

H = –14.285 kJ/mol	h = 2120.7 J/(mol·K)
S = –11.53 J/(mol·K)	s = –2.96 J/(mol·K)

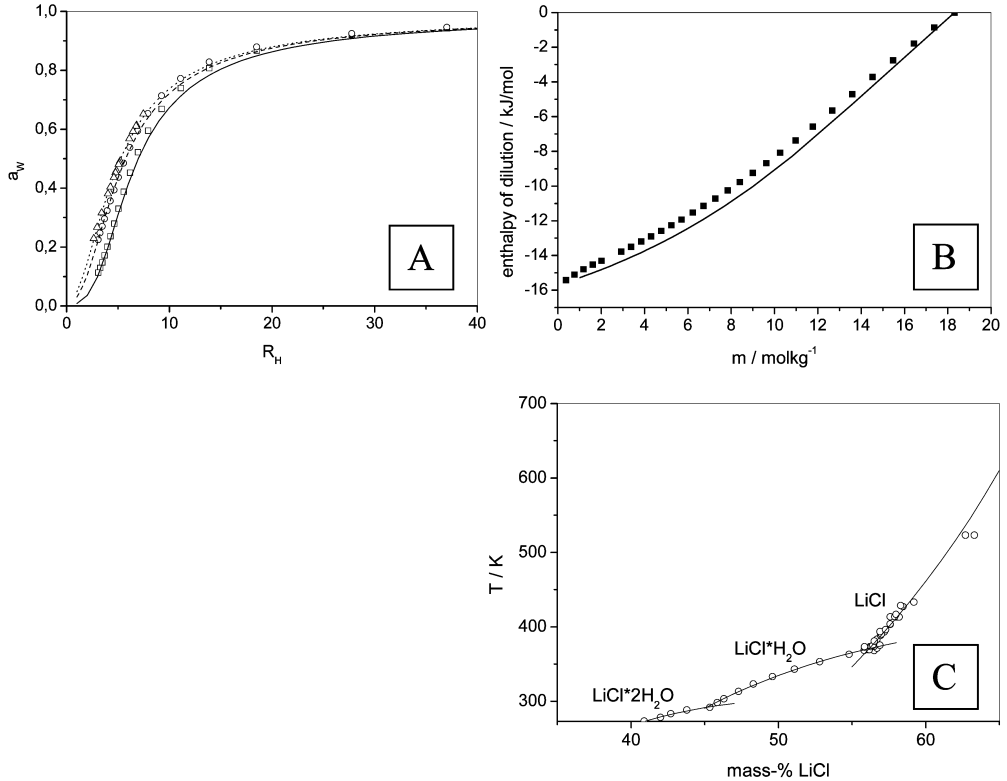

Fig. 6 System LiCl–H_2O. (A) Water activity (□ 298 K [24]), (○ 373 K [25]), (△ 428 K); (B) Enthalpy of dilution at 298 K, $m_{initial}$ = 18.3 mol/kg H_2O [26]; (C) Solid–liquid phase diagram LiCl–H_2O [27].

From spectroscopic investigations in highly concentrated aqueous solutions of zinc chloride, a large number of tetrahedral and octahedral coordinated species is discussed in literature within different ranges of composition and temperature. Most important species seem to be $Zn(H_2O)_6^{++}$, $ZnCl_2(H_2O)_2$, and $ZnCl_4^{2-}$, however, also other stoichiometries like $ZnCl_3(H_2O)^-$ or $ZnCl(H_2O)_5^+$ are reported. Available measurements of water activities, heats of dilution, and heats of mixing in the systems $ZnCl_2$–H_2O and LiCl–$ZnCl_2$–H_2O are reasonable reproduced formulating species of a reaction scheme as given in Fig. 7. Thereby, species like $ZnCl_4(H_2O)_2^{2-}$ should rather be considered as a secondary hydrated tetrahedral $ZnCl_4^{2-}$ than an octahedral complex ion. Using this model with parameters as listed in Table 3, the experimental data of the phase diagram LiCl–$ZnCl_2$–H_2O have been described correctly at 298 and 313 K (Fig. 8). $ZnCl_2$, H_2O, and Cl^- are assumed as basis species with values of H^0 and S^0 set to zero at all temperatures. Since enthalpy data had been included in parameter estimation predictions of solid–liquid equilibria at other temperatures have a solid basis.

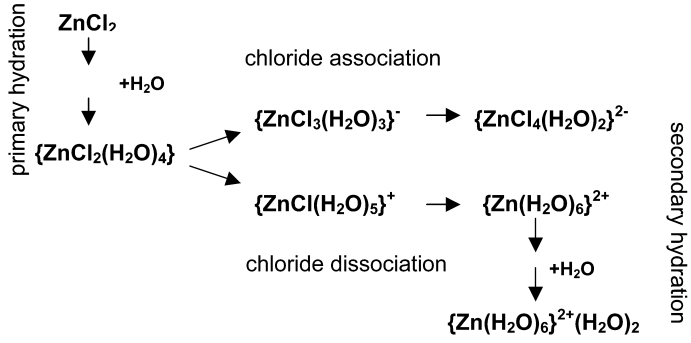

Fig. 7 Formation scheme of zinc-containing species.

Table 3 Model parameters for liquidus species and solid phases in the system LiCl–$ZnCl_2$–H_2O.

Species	H^0	S^0	Species	H^0	S^0
	kJ/mol	J/(mol·K)		kJ / mol	J/(mol·K)
$ZnCl_2(H_2O)$	–75.90	–18	$ZnCl_4(H_2O)_2^{2-}$	–106.91	64
$ZnCl_2(H_2O)_2$	–90.73	–36	$ZnCl(H_2O)_5^+$	–77.49	–72
$ZnCl_2(H_2O)_3$	–101.91	–54	$Zn(H_2O)_6^{2+}$	–114.93	–230
$ZnCl_2(H_2O)_4$	–109.50	–72	$Zn(H_2O)_6(H_2O)^{2+}$	–126.50	–262
$ZnCl_3(H_2O)_3^-$	–87.68	–4	$Zn(H_2O)_6(H_2O)_2^{2+}$	–138.25	–294
Solids			Solids		
$ZnCl_2$(s)	–101.78	–120	$LiCl{\cdot}2H_2O$(s)	–40.52	–58.5
LiCl(s)	–13.04	–6.8	$LiCl{\cdot}ZnCl_2{\cdot}2.5H_2O$(s)	–280.18	–450
$LiCl{\cdot}H_2O$(s)	–29.63	–39			

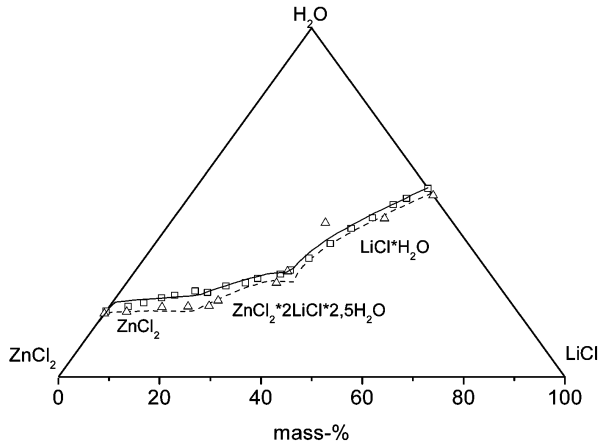

Fig. 8 Solubility curves in the system LiCl–$ZnCl_2$–H_2O at 298 and 313 K. Lines: calculated; symbols: experimental data [2].

The application of this approach to other systems like KCl–$MgCl_2$–H_2O and $MgCl_2$–$CuCl_2$–H_2O is described elsewhere [20].

CONCLUSION

Applications of salt hydrates require fine-tuned melting temperatures, which can be achieved by using mixtures. For predictions of suited eutectic mixtures, two approaches have been proved successfully to calculate polythermal phase diagrams from a limited amount of thermodynamic and phase equilibria data. The BET approach is recommended for simple mixtures and a reaction chain approach for mixtures characterized by extensive complex ion formation. Phase diagrams predicted in this way provide guidance for later experimental work.

ACKNOWLEDGMENTS

The authors wish to thank DFG ("Deutsche Forschungsgemeinschaft" within the program "Stoffeigenschaften komplexer fluider Gemische", project Vo 644/2) and Merck KGaA Darmstadt for financial support.

REFERENCES

1. A. I. Kirgintsev, L. I. Trushnikova, V. G. Lavrent'eva. "Solubility od inorganic substances", Izd. Khimiya, Leningrad (1972).
2. W. F. Linke and A. Seidell. *Solubilities: Inorganic and Metal-Organic Compounds*, American Chemical Society, Washington, DC (1965).
3. K. S. Pitzer. *Activity Coefficients in Electrolyte Solutions*, 2nd ed. CRC Press, Boca Raton, FL (1991).
4. J. Braunstein. In *Ionic Interactions*, Vol. 1, S. Petrucci (Ed.), Academic Press, New York (1971).
5. R. H. Stokes and R. A. Robinson. *J. Am. Chem. Soc.* **70**, 1870 (1948).
6. M.-C. Trudelle, M. Abraham, J. Sangster. *Can. J. Chem.* **55**, 1713 (1977).
7. C. B. Richardson and C. A. Kurtz. *J. Am. Chem. Soc.* **106**, 6615 (1984).
8. G. A. Sacchetto and Z. Kodejs. *J. Chem. Soc., Faraday Trans. 1* **84**, 2885 (1988).
9. W. Voigt. *Monatsh. Chem*. **124**, 839 (1993).

10. J. Braunstein and M. R. Ally. *Monatsh. Chem*. **127**, 269 (1996).
11. M.-C. Abraham, M. Abraham, J. Sangster. *J. Chem. Eng. Data* **25**, 331 (1980).
12. J. Sangster, M.-C. Abraham, M. Abraham. *Can. J. Chem*. **56**, 348 (1978).
13. M. R. Ally and J. Braunstein. *J. Chem. Thermodyn*. **30**, 49 (1998).
14. E. M. Kristiansen. "Molten salt hydrates for heat storage applications", Master's Thesis, University of Science and Technology, Trondheim (1994).
15. J. Heckenkamp and H. Baumann. *Nachr. Chem. Tech. Lab*. **45**, 1075 (1997).
16. R. H. Stokes and R. A. Robinson. *J. Solution Chem*. **2**, 173 (1973).
17. ChemSage: GTT-Technologies, Kaiserstrasse 10, D-52134 Herzogenrath, Germany.
18. T. J. Wolery. "EQ3/6, a computer program for geochemical aqueous speciation-solubility calculations: Theoretical manual, user's guide, and related documentation", Lawrence Livermore National Laboratory (1992).
19. A. R. Conn, N. I. M. Gould, P. L. Toint. "Lancelot: A Fortran package for large-scale nonlinear optimisation", Springer-Verlag, Berlin (1992).
20. W. Voigt and D. Zeng. "Ion coordination and thermodynamic modelling of molten salt hydrate mixtures", in *Properties of Complex Fluid Mixtures*, Wiley-VCH, New York (2002). In press.
21. B. E. Conway. *Ionic Hydration in Chemistry and Biophysics*, Elsevier, Amsterdam (1981).
22. M. Peschke, A. T. Blades, P. Kebarle. *J. Phys. Chem. A* 9978 (1998).
23. M. Peschke, A. T. Blades, P. Kebarle. *Intern. J. Mass Spectrosc*. 685 (1999).
24. J. A. Rard and D. G. Miller. *J. Chem. Eng. Data* **26**, 38 (1981).
25. V. Brendler. "Wasseraktivitäten in den binären Systemen $MgCl_2$–ACl–H_2O (A = Li, K, Cs) bis zu sehr hohen Salzkonzentrationen", Ph.D. thesis, TU Bergakademie, Freiberg.
26. E. Lange and F. Duerr. *Z. Phys. Chem. (Leipzig)* **126**, 361 (1926).
27. R. Cohen-Adad and J. W. Lorimer. *Solubility Data Series: Alkali Metal and Ammonium Chlorides in Water and Heavy Water (Binary Systems)*, Vol. 47, Pergamon Press, Oxford (1992).
28. St. Tepavitcharova, Chr. Balarev, St. Trendafilova. *J. Solid State Chem*. **114**, 385 (1995).